RSC Advances

This article can be cited before page numbers have been issued, to do this please use: X. Wu, X. Xia, Y. Chen and Y. Lu, *RSC Adv.*, 2016, DOI: 10.1039/C6RA15161B.

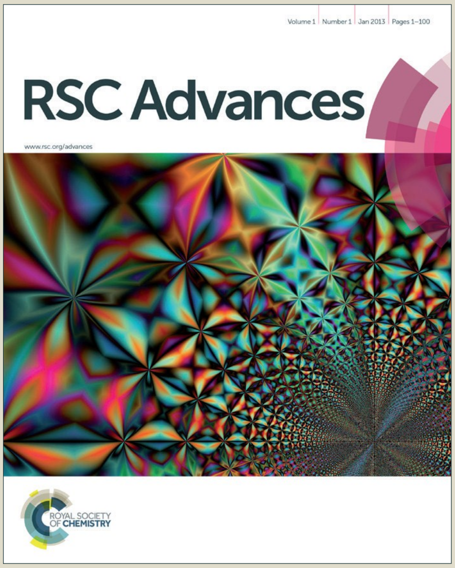

View Article Online
DOI: 10.1039/C6RA15161B

RSC Advances

ARTICLE

Mesoporous Al-incorporated silica-pillared clay interlayer materials for catalytic hydroxyalkylation of phenol to bisphenol F

Xianzhang Wu, Xinnian Xia*, You Chen and Yanbing Lu

Received 00th January 20xx,
Accepted 00th January 20xx

DOI: 10.1039/x0xx00000x

www.rsc.org/

A series of mesoporous Al-incorporated silica-pillared clay (Al-SPCs) interlayer materials with different Al content were prepared in the presence of cationic surfactant by structure-directing method. The catalysts structure, texture, and acidic properties were determined using XRD, BET, SEM, TEM, FT-IR, NH_3-TPD and Py-IR, respectively. Characterization results showed that these materials possess mesoporous structure with large specific surface areas. The incorporated Al leading to the increase and redistribution of Brönsted and Lewis acid sites on SPC (silica-pillared clay). The Al-SPCs were used as catalysts for hydroxyalkylation of phenol to bisphenol F, and give a high product yield (95.4%) and selectivity (98.2%) to bisphenol F. Catalytic performance of the catalysts and characterization results proved that the catalytic activity of these catalysts depended on moderate acidity and the textural properties (specific surface areas). Meanwhile, the synergy of Brönsted acid and Lewis acid is key for hydroxyalkylation of phenol to bisphenol F. The reusability of the catalyst was studied, which the catalysts can be easily recovered and reused for at least six times without significant loss of their catalytic activities. Finally, a plausible mechanistic pathway was proposed.

1 Introduction

With increasing demand and applicability in plastics, resins and rubber industries, bisphenol F synthesis has been given an extensive attention. Synthesis of bisphenol F via hydroxyalkylation of phenol with formaldehyde is a typical acid-catalyzed reaction. Classically, hydroxyalkylation of phenol with formaldehyde to bisphenol F could be catalyzed by use of various conventional mineral acids, such as phosphoric acid, hydrochloric acid, sulfuric acid or other inorganic acids.[1] Even though moderate to high bisphenol F yields have been achieved, sustainable and economically viable routes for bisphenol F production in scalable quantities arose serious challenges due to these are toxic, corrosive, and often hard to remove from the reaction solution. Thus, it is keenly desirable to develop new types of catalysts to replace them. The solid catalysts were well recognized these days because of their ease of workup, separation of products and catalysts, and economical advantages. More importantly, it has unique properties including availability, safety, nontoxicity, and insolubility in the vast majority of solvents. Because of these properties, a number of studies have been reported about the design of solid acid catalysts for bisphenol F synthesis, which spans over a broad range of catalytic materials including modified mesoporous silicas,[2] clay,[3] organometallic framework,[4] and zeolites[5]. Recently, Chen et al.[6] reported the metal–organic frameworks of MIL-100(Fe or Cr) and MIL-101(Fe or Cr) encapsulated with Keggin phosphotungstic acid as a catalyst for hydroxyalkylation of phenol to form bisphenol F. The studies indicate that the nature of the transition metal Fe or Cr in MIL-100 or MIL-101 material determined the isomers' distribution of bisphenol F. Even though the materials formed are good catalysts for hydroxyalkylation of phenol to bisphenol F, the synthesis procedure is somewhat tedious. Garade et al.[7] reported, for the first time, that DTP/SiO_2 was active for bisphenol F synthesis. However, the yield of bisphenol F was only 34.2%, which the low catalytic activity severely restricted its application. It is desirable to develop a cheaper and easier to synthesize catalysts for hydroxyalkylation of phenol with formaldehyde to bisphenol F.

Pillared clay (PILC) is one of the most widely studied interlayer materials, which have potentially wide applications in the areas of adsorption and catalysis. [8-10] The introduction of oxide pillars into the interlayer space results in a significant increase in surface area, thermal stability, and microporosity. More importantly, by changing the pillar oxide and raw clay, the acidity, layer space, and pore size distribution of the PILCs can be regulated over relatively wide ranges. Pillared clay are suited to be used in heterogeneous liquid phase reactions, offering new opportunities for developing environmentally benign and friendly processes. In this article, a series of Al-SPC with different contents of Al were synthesized, and catalytic performance of the Al-SPCs for hydroxyalkylation of phenol to bisphenol F was studied in detail. An Al-pillared montmorillonite (Al-MMT) was also prepared and used as a catalyst for comparative purposes. The experimental results are well explained based on characterization by X-ray diffraction (XRD), FT-IR using pyridine as a probe (Py-IR), and NH_3 temperature programmed desorption (NH_3-TPD).Also, the reusability of the catalyst were investigated; As well, reaction parameters such as catalyst weight, reaction temperature, reaction time and molar ratio were optimized.

College of Chemistry and Chemical Engineering, Hunan University, Changsha 410082, P. R. China. E-mail: xnxia@hnu.edu.cn; Fax: +86 731 88821549; Tel: +86 73188821549

View Article Online
DOI: 10.1039/C6RA15161B

2 Experimental

2.1 Materials

Commercially available montmorillonite K10 as the raw Material supplied by Sinopharm Chemical Reagent Co, Ltd, China. Analysis of its mineralogy composition showed it to be 95% montmorillonite. Its anhydrous structural (layer) formula, which was determined previously[11] is as $[Si_{7.86}Al_{0.14}][Al_{2.84}Fe_{0.30}Mg_{0.86}]O_{20}(OH)_4$. Montmorillonite K10, which is calcium-rich in commodities form and was converted into the Na-MMT (denoted as MMT) by treatment with NaCl (1 mol/L NaCl solution, 100 mL solution/g of clay, 80℃ for 2 h); Dodecyl dimethyl benzyl ammonium chloride (C_{12}DMBACl) (A.R.),Tetraethoxysilane (TEOS) (A.R.), ammonia (25%) Ethanol (99.7%) was purchased from Beijing Chemical Reagents Company, China. phenol, formaldehyde (37–40%), aluminum chloride hexahydratere ($AlCl_3{\cdot}6H_2O$) were purchased from Sinopharm Chemical Reagent Co, Ltd, China.

2.2 Synthesis of SPC

SPC were synthesized in the presence of cationic surfactant by structure-directing method according to previous report.[12] Typically, MMT (1.00 g) was added to 30 mL of water to form a clay suspension. C_{12}DMBACl was dissolved in ethanol, and TEOS was added and stirred for 0.5 h to form a clear solution. The solution was then slowly dropped into the clay suspension. The gel mixture with a molar ratio of clay, surfactant, TEOS, ethanol and water at 1:2:30:1.2:250 was stirred for 0.5 h. Subsequently, the mixture was filtered to remove the water and extra TEOS, and the product obtained was C_{12}DMBACl/TEOS-intercalated clay.

The C_{12}DMBACl/TEOS-intercalated clay (2.g) was dispersed in 50 mL of ammonia solution and stirring for 2 h at room temperature. The resultant mixture was subsequently separated from suspension by filtration to obtain powders, dried in an air and calcined at 600 ℃ for 3 h (at a heating rate of 2℃/min) to remove C_{12}DMBACl. The prepared sample was denoted as SPC.

2.3 Synthesis of Al-SPCs

Al-SPCs was prepared in the presence of cationic surfactant by structure-directing method as follows:(i) MMT (1.00 g) was suspended in 30 mL of water to form suspension A. (ii) $AlCl_3{\cdot}6H_2O$ (1.2g) was added to a solution consisting of 2 mL of ethanol and 8 mL of TEOS to form suspension B. (iii) The suspension B was slowly dropped into suspension A, and stirred for 1h to obtain a brown sol. Then, 3 mL of ammonia solution was slowly dropped into the sol and stirring for 3 h at room temperature. The resultant mixture was subsequently separated from suspension by filtration to obtain powders, dried in an air and calcined at 600 ℃ for 6 h using a programmed furnace (at a heating rate of 2℃/min). The product was denoted as Al-SPC-X, where the X represents the molar of Al in per gram of MMT.

2.4 Synthesis of Al-MMT

Al-MMT was synthesized by intercalation of Na-MM with aluminum hydroxy oligomeric solutions (Al solutions) according to our previous reports.[13] 0.1 mol/L solution of NaOH was slowly added to 0.1 mol/L $AlC1_3$ solutions prepared from $AlCl_3{\cdot}6H_2O$ to obtain a final hydrolysis ratio OH^-/Al^{3+} = 2.4. Aging at 50℃for 24 h, the $AlC1_3$ solution was slowly added to MMT slurry of 2g/100 ml (10 mmol of Al per gram of MMT). The final suspension was stirred at room temperature for 24 h, then was transferred to dialysis tubing and dialyzed in distilled water for 3 days to remove $C1^-$. The dialysis water was changed each 24 h until the water-tested $C1^-$ free by the $AgNO_3$ test. The resultant mixture was subsequently separated from suspension by filtration to obtain powders, dried in an air and calcined at 400 ℃ for 4 h.

2.5 Catalytic activity tests.

Hydroxyalkylation of phenol with formaldehyde to bisphenol F was performed in a magnetically stirred glass reactor fitted with a reflux condenser and an arrangement for temperature control under nitrogen atmosphere. Briefly, 82.86 mmol of phenol, 5.73 mmol of formaldehyde and catalyst (0.12 g) were added into the glass reactor. The reaction mixture was magnetically stirred and heated to the required temperature. After a definite time interval, the reaction is stopped and 0.03 g of the product is taken and is diluted with 10 mL of methanol. The products were analyzed by a HPLC system with a Shimadzu LC-20AT system coupled with a SPD-20A UV/Vis detector and a Phenomenex Luna C18 column (250 × 4.6 mm, 5 μm) and Column oven temperature was 25℃, and mobile phase was methanol : water with 65:35v/v. mobile phase whose flow was 0.6 mL/min.

The reaction equation of phenol with formaldehyde to bisphenol F is shown in Scheme 1.

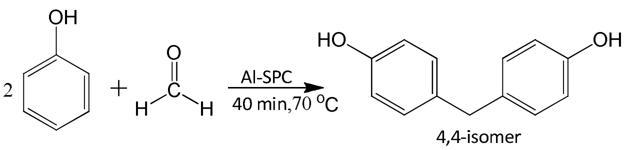

Scheme 1. Hydroxyalkylation of phenol with formaldehyde to bisphenol F.

The yield and selectivity of bisphenol F were calculated on the basis of formaldehyde. The calculation equations are as follows:

$$\text{Yield}\,(\%) = \frac{\text{moles of bisphenol F}}{\text{moles of HCHO charged}} \times 100\%$$

$$\text{Selectivity}\,(\%) = \frac{\text{moles of bisphenol F formed}}{\sum \text{moles of all the products}} \times 100\%$$

2.6 Catalyst Characterization.

Powder X-ray diffraction (XRD) patterns were recorded at room temperature on a D8-Advance with Cu Kα radiation (λ = 0.1541 nm) at 40 kV and 40 mA. Diffraction data were recorded in the 2 h range from 1° to 8° and 10° to 80° with a scanning rate of 0.5° of 2θ/s and 2θ = 0.02°. Scanning electron microscopy (SEM) micrographs were obtained on a Hitachi S-4800 microscope operated at 30 kV. The chemical composition of the sample was determined by energy-dispersive X-ray (EDX) analysis using an FEI QUANTA-200. Transmission electron microscope (TEM) images were obtained using a JEOL JEM-2100 microscope. The TEM samples were prepared by dispersing nanoparticles in acetone to form a suspension. The suspension was sonicated for 20 min and was

View Article Online
DOI: 10.1039/C6RA15161B

deposited onto Cu grid with lacey carbon coated.NH_3-TPD analysis was performed with a Micromeritics AutoChem II 2920 V3.05 instrument. Prior to analysis, the catalyst (100 mg) was enclosed in a quartz tube and treated at 300 ℃ under a helium flow of 30 mL/min for 1 h. The sample was cooled down to 60℃ under a flow of helium gas and then followed by adsorption of NH_3 for 60 min, which was maintained for 1 h. Subsequently, the catalyst was heated to 700 ℃ with a ramp of 10 ℃/min under a helium flow rate of 30 mL/min. A thermal conductive detector (TCD) was used to measure the desorption amount of NH_3 which was quantified based on the TCD calibration curve that had been obtained by injecting NH_3 pulses of known volume in the helium background flow.

Pyridine adsorption monitored by in situ infrared FTIR spectra (Py-IR) of the catalyst samples were recorded with a Brucker Vector 22 spectrometer in the absorption mode with a resolution of 4 cm^{-1}. Self-supporting wafers were made and loaded in an IR cell. The wafers were pretreated at 400℃ under flowing oxygen for 2 h. Background spectra were recorded after the sample was cooled to room temperature. Adsorption of pyridine was then conducted until saturation. Py-IR spectra were recorded after degassing for 0.5 h. The specific surface area was estimated according to the Brunauer−Emmett−Teller (BET) equation. The pore size distribution was calculated by the Barett−Joyner−Halenda (BJH) method by the adsorption isotherm branch. Infrared spectra were recorded in the wavelength range of 800–4000 cm^{-1} using a Bruker vector 22 FT-IR spectrophotometer using KBr disk technique.

3 Results and discussion

3.1 Catalyst characterization

Fig. 1(A) shows small-angle XRD patterns of SPC, Al-SPCs and Al-MMT. As can be seen in SPC and Al-SPCs, these reflections were very similar, indicating that all of samples had similar basal spacings and lamellar structures by this synthesis method.[14] However, for Al-MMT, the 001 reflection peak is shifted toward higher diffraction angles, and exhibits lower intensity, illustrating that Al-MMT prepared by Al pillared MMT has a smaller layer spacing than Al-SPCs. The basal spacing values, for the montmorillonite component in both the MMT, Al-SPCs and Al-MMT catalyst are shown in Table 1. The basal spacing increases from 1.7 nm in the MMT to 3.16 nm in the Al-SPCs. This results is expected because of expansion of the interlayer spacing in the MMT after pillaring treatment, indicating that SiO_2 has been successfully intercalated into the clay layers.[15] The basal spacing of Al-MMT is 2.1 nm, which smaller than Al-SPCs. Interestingly, no significant difference in the intensities among the 001 refraction peaks between SPC and Al-SPCs was observed, suggesting that the amount of Al element used does not affect the layered structure of Al-SPCs.

The wide-angle XRD patterns of MMT, SPC, Al-SPCs and Al-MMT are presented in Fig. 1(B). All the samples shows the typical peaks of the trioctahedral subgroup of 2:1 phyllosilicates, which are ascribed to (110), (020), (004), (130), (200), (330) and (060) diffractions.[16] It is seen that there are no diffraction lines in Fig. 1(B), indicating that Al species well-dispersed in the interlayered silica oxide framework and no long-range change in the crystalline structure of clay.

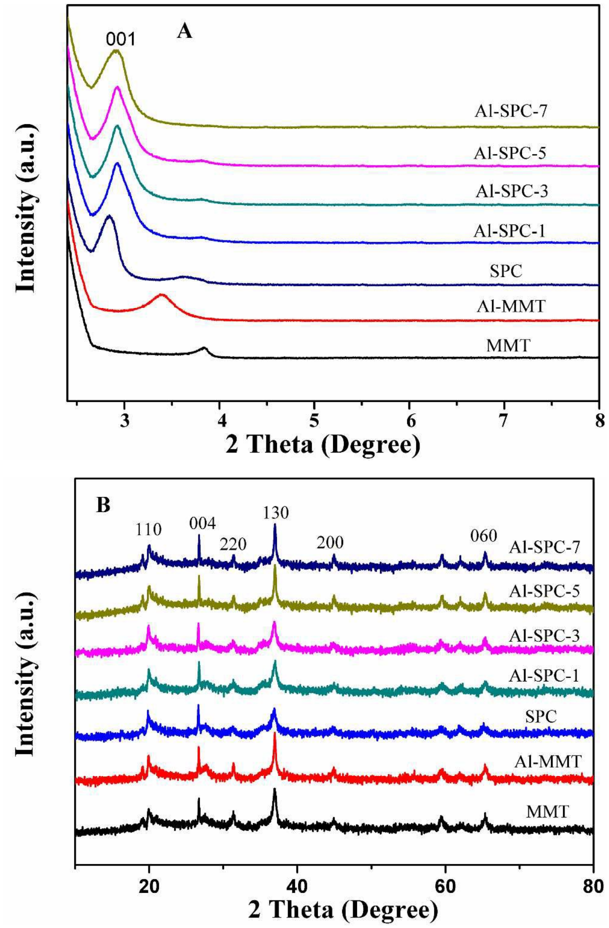

Fig. 1 XRD patterns of SPC, Al-SPCs and Al-MMT samples.

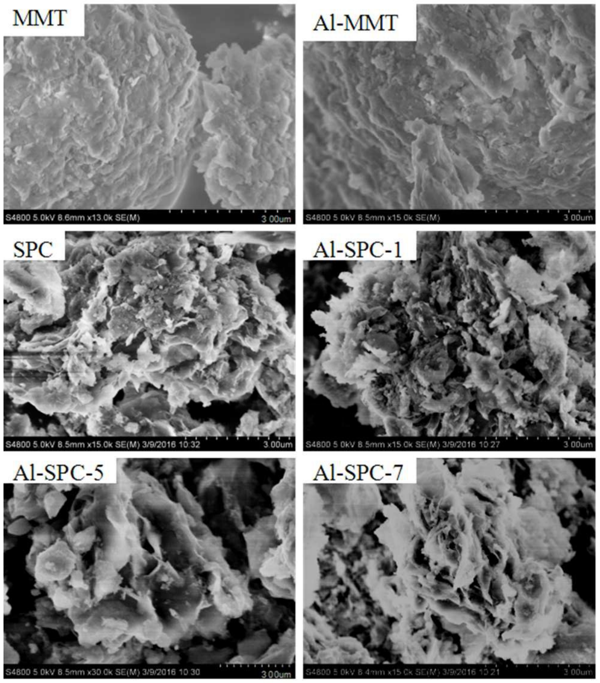

Fig. 2 SEM image of SPC, Al-SPCs and Al-MMT samples.

View Article Online
DOI: 10.1039/C6RA15161B

Table 1. Structural data of the samples.

samples	Surface area ($m^2 g^{-1}$)	basal spacing (nm)	gallery height (nm)	Pore volume ($cm^3 g^{-1}$)	pore size (nm)	Al content (wt %)
MMT	61	1.7	0.74	0.12	7.4	12.6
SPC	657.8	3.16	2.16	0.76	12.5	10.5
Al-SPC-1	584.6	3.13	2.13	0.72	12.2	15.7
Al-SPC-3	475.2	3.12	2.16	0.63	12.1	21.1
Al-SPC-5	410.9	3.12	2.21	0.54	12.2	27.2
Al-SPC-7	386.3	3.12	2.21	0.32	12.1	32.6
Al-MMT	207.5	2.14	2.20	0.35	10.4	34.9

The SEM micrographs were used to further study the structural information of the catalyst. As shown in the Fig. 2. The MMT and Al-MMT show a closer sheets structure, owing to that the MMT and Al-MMT possesses ordered layered structure and small layer spacing. The platelets in the SPC and Al-SPCs were unaffected by hydrolysis, although they swelled slightly more than the MMT and Al-MMT. All of the Al-SPCs derivatives synthesized using cationic surfactants exhibited similar morphologies. Moreover, some small particles can be observed around platelets of SPC and Al-SPCs. This is due to the broken platelets and the forming of some compounds in the extralayer regions of the clays.[17] However, this platelet destruction did not reflect SPC and Al-SPCs gallery structure destruction .This result is confirmed by XRD Spectra.

FT-IR patterns of MMT, SPC, Al-SPCs and Al-MMT are shown in Fig. 3. The absorption bands at about 3450 and 1658 cm^{-1} were assigned to the stretching and bending vibrations of the O-H bond in the clay and water molecules present in the interlayer.[18] In all curve, the band at around 3652 cm^{-1} is due to the vibration of Al-OH. Typical bands of the silicate components appear between 1300 and 800 cm^{-1}, and the absorption at 852 cm^{-1} is due to the Si-OH in the tetrahedral layer.[19] The band located at 1028 cm^{-1} was indexed to the asymmetric stretching bonds of Si-O-Si.[20] Compared to the FT-IR spectra of pure MMT and SPC, significant increase of the peaks intensity at 36542 cm^{-1} with increasing content of Al in Al-SPCs, which is attributable to the appearance of Al-OH bending vibration and the intensity is also enhanced. The above results revealed that Al atoms were incorporated into the interlayered framework of clay.

To get further insight into the layered structure of Al-SPCs, HRTEM investigations were then conducted and the corresponding images are shown in Fig 4.The HRTEM image (Fig 4A) of MMT shows that the sheets keep together closely. From the image (Fig 4B and 4D) of the SPC and Al-SPC-7, clear solid dark lines and the pores can be observed, which is attributable to the clay layers.[21] Furthermore, the uniform gallery pores can be clearly observed between the dark layers. Obviously, the Al-SPC-5 (Fig 4C) shows the uniform layered structure, and has relative higher gallery height than MMT.

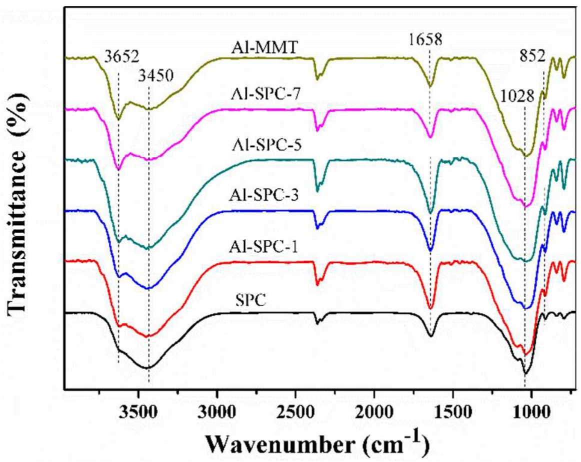

Fig. 3 FT-IR spectra of SPC, Al-SPCs and Al-MMT samples.

The N_2 adsorption-desorption isotherms of the SPC, Al-SPCs and Al-MMT are presented in Fig. 5(A) and average pore dimensions and volumes obtained from the maxima (BJH) are presented in Table 1.Irrespective of treatment method, the N_2 isotherms of the catalysts can be assigned to be a combination of types I and IV[22] according to the BDDT (Brunauer, Deming, Deming, and Teller) classification, and the features of hysteresis loop correspond to the type B in Boer's five types, suggesting that the presence of the open slit-shaped capillaries with very wide bodies and narrow short necks in the region between interlayers.[23] Compared with MMT and Al-MMT, the SPC and Al-SPCs have a significant increase in porosity

View Article Online
DOI: 10.1039/C6RA15161B

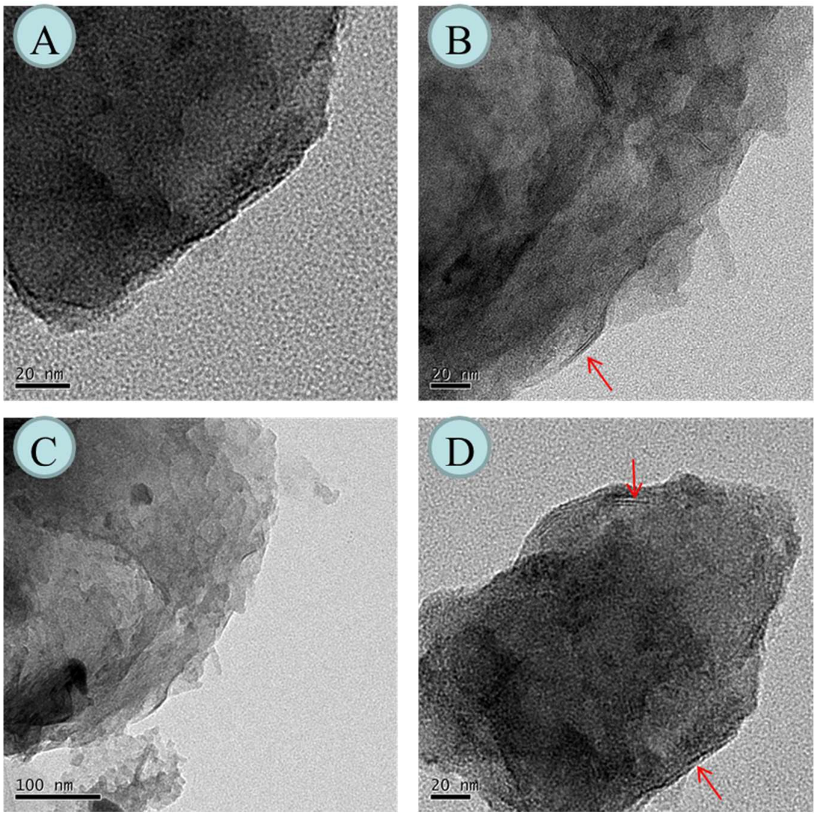

Fig 4. HRTEM images of (A) MMT, (B) SPC, (C) Al-SPC-5 and (D) Al-SPC-7 sample.

and surface area, which is attributable to the forming of rigid intercalated porous structure when TEOS that as the pillaring precursors are converted to firm enough silica pillars. As shown in Fig. 4(A), the slight increase in the amount of N_2 adsorbed with increasing relative pressure from a low to a medium value (P/P_o =0.01–0.2) indicating that these materials possess supermicropores and small mesopores.[24] In the P/P_o region from 0.0 to 0.4, the adsorption isotherm gives a good fit with the BET equation as well as with the Langmuir equation; The above results indicates that the pores formed between parallel layers are quite open.

The BJH-adsorption pore size distribution curves of the samples are shown in Fig. 4(B). All the Al-SPCs studied displayed different mesopore size distributions. The average pore size of Al-SPCs was 12.1-12.2 nm, which was slightly less than the average pore size of SPC, indicating that the interlayer frameworkthe are changed by incorporation of Al. It might be owing to the extragallery Al_2O_3 occupied the spaces of gallery channels and increased the thickness of the pore walls, and resulting in a slightly decreased of the average pore size. These results were in great agreement with the N_2 adsorption–desorption isotherms. The average pore size of SPC is closely related to the interlayer space height. This implies that the interlayer surfactant plays an important structure-directing role in the synthesis of the intercalated silica. The surface area and pore volume of the Al-SPCs decreased with increase in as the content of Al (Table 1), which is owing to the packing of small metal particles on the surfaces and pores.[25]

NH_3-TPD analysis was performed in order to evaluate the quantification of the catalysts acid density and the results are shown in Fig. 5. The amount of surface acid sites based on NH_3 desorption are presented in Table 2. From Fig. 5, three types of desorption peaks from 99 to 530℃region was observed, which could be denoted as weak, moderate and strong acid sites, respectively.[26] The weak and moderate acid sites in the form of the OH groups bonded to the pillars Al ions (Al–OH), and the strong acid sites is associated with the OH groups bonded to tetrahedrally coordinated Al ions (Al_{Td}–OH). [27] As the Al content increased from 1 to 7, the total amount of acid sites of Al-SPCs significantly increased. Meanwhile, the amount of moderate acid sites of Al-SPCs enhanced considerably from 1.90 to

View Article Online
DOI: 10.1039/C6RA15161B

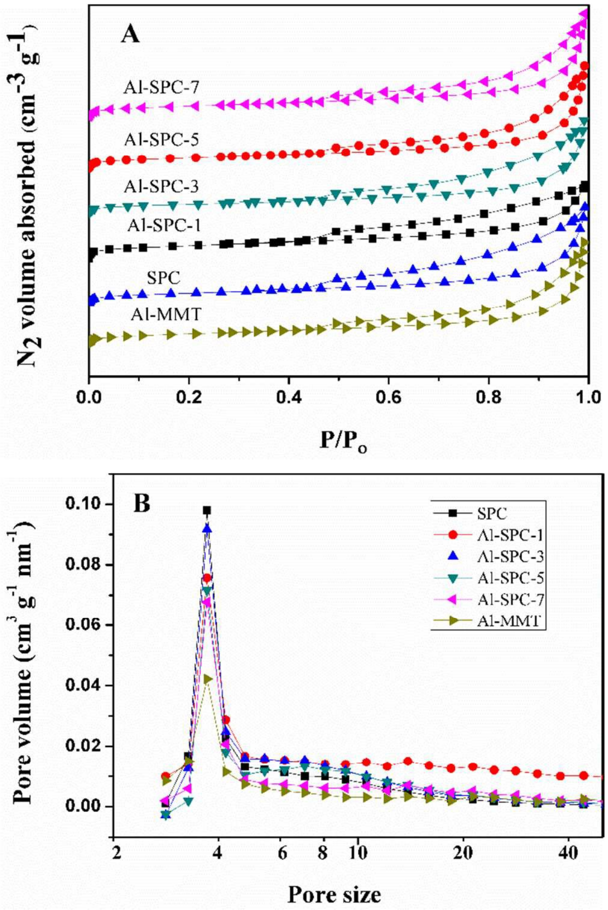

Fig .5 N_2 adsorption–desorption curves (A) and pore size distributions (B) of SPC, Al-SPCs and Al-MMT samples.

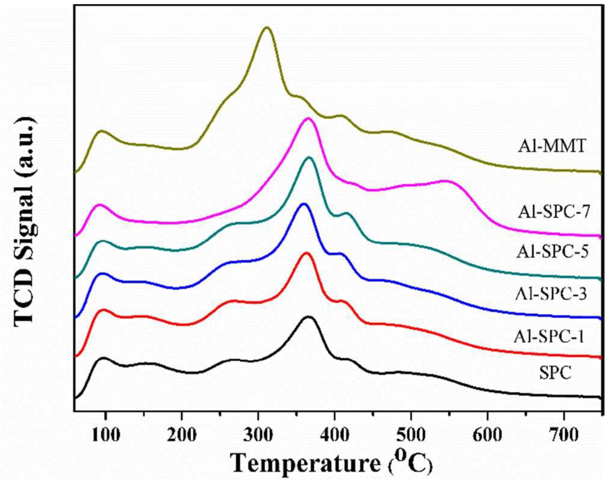

Fig. 6 NH_3-TPD profiles of SPC, Al-SPCs and Al-MMT samples.

3.19 mmol g^{-1}. Interestingly, the amount of weak and strong acid sites only shows a minor change. In addition, the highest amount of moderate acid sites were found in Al-MMT, which may due to high Al content for Al-MMT.

The acid properties of SPC and Al-SPCs and were evaluated by FT-IR measurement for samples with adsorbed pyridine and the results are shown in Fig. 7. The amounts of Brönsted and Lewis acid sites are listed in Table 2. These peaks could be assigned to the chemisorption of molecular pyridine at different type of surface acidic sites. The band at 1447 cm^{-1} in the difference FT-IR spectra in Fig. 7 is assignable to coordinated pyridine species with Lewis acid sites.[28] The band at 1544 cm^{-1} due to pyridinium ions bonded to Brönsted acid sites. The band at 1490 cm^{-1} attributed to pyridine associated with both Lewis and Brönsted acid sites.[29-30] It can clearly found that only small peaks corresponding to pyridine adsorbed on acidic sites were observed for SPC, indicating that the surface acidities of SPC were weak. Meanwhile, the amounts of Brönsted and Lewis acid sites on Al-SPCs increased from 0.18 to 0.32 mmol g^{-1}, and 0.13 to 0.53 mmol g^{-1} with increase in Al content from1 to 7, respectively. Note that Al significantly affected the acidity of the MMT materials and the addition of Al resulted in the increase and redistribution of the two types of acid sites. Moreover, this results shows that Al-SPCs, which was highly active for the reaction result from higher L/B ratio. Therefore, the hydroxyalkylation of phenol to bisphenol F is catalyzed by the synergy of Brönsted acid and Lewis acid rather than a single one. This results was confirmed by Py-IR results and is well consistent with the above NH_3-TPD result.

As shown in the Scheme 2, Al was incorporated in the silica-framework between the interlayer regions of MMT.

3.2 Activity measurement

The catalytic activity of the prepared SPC, Al-SPCs and Al-MMT were evaluated for the hydroxyalkylation of phenol. The results are summarized in Table 3. As compared to MMT and SPC, Al-SPCs shows of Aluminum species presence in the gallery silica framework. Obviously, Al-SPC-5 had the highest activity (95.4%), higher than that very high catalytic activity, indicating that catalytic activity is a result

Table 2. Acidic properties of various solid acid catalysts.

	NH_3-TPD amount of acidic sites (mmol g^{-1})				Acidity by type (mmol g^{-1})		
Catalyst	Weak	Moderate	Strong	Total	Brönsted	Lewis	Lewis/Brönsted
SPC	0.49	1.90	1.11	3.50	0.18	0.13	0.72
Al-SPC-1	0.50	2.05	1.09	3.64	0.25	0.23	0.92
Al-SPC-3	0.51	2.27	1.06	3.84	0.27	0.26	0.96
Al-SPC-5	0.54	2.92	1.10	4.56	0.29	0.41	1.41
Al-SPC-7	0.56	3.19	1.93	5.68	0.32	0.53	1.66
Al-MMT	0.62	4.60	1.02	6.24	—	—	—

View Article Online
DOI: 10.1039/C6RA15161B

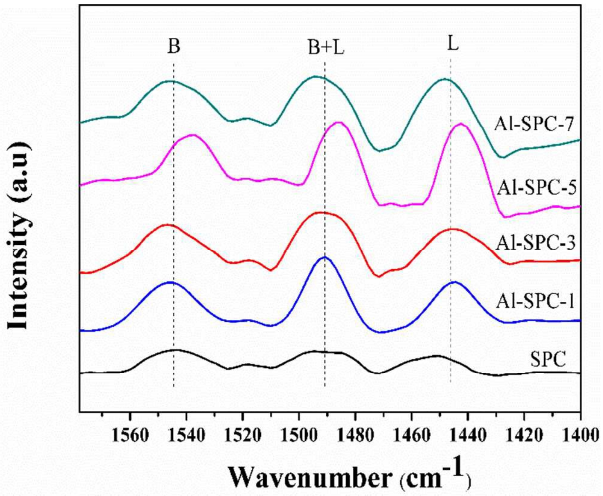

Fig. 7 Py-IR spectra of SPC and Al-SPCs samples.

of the Al-SPC-3 catalyst (72.8%). With the increase of Al content from 1 to 5, the bisphenol F yield increasing from 36.5 to 95.4%. This is attribute to enhanced amount of moderate acid sites and higher L/B ratio resulted in higher catalytic activity, which is confirmed the results of NH_3-TPD and Py-IR (Table 2). When further increase in Al content up to 7, there is a decrease of bisphenol F yield (94.7%). This may be due to the Al-SPCs derivatives prepared with high Al content contain mainly isolated tetracoordinated Al species incorporated in the gallery silica structure, which leads to a gradual reduction of quality of pore structure and of the pore volumes and results in decline of specific surface areas. Interestingly, the Al-MMT show the lower catalytic activity than Al-SPC-5 and Al-SPC-7, although it has the higher amount of moderate acid sites. This is attribute to the low specific surface areas of Al-MMT. These experimental results were in good agreement with the NH_3-TPD analysis and the N_2 adsorption- desorption isotherms, indicating that the catalytic activity is good agreement with the NH_3-TPD analysis and the N_2 adsorption- desorption isotherms, indicating that the catalytic activity is dependent on the amount of moderate acid sites and the specific surface area of catalyst for the hydroxyalkylation of phenol. Al-SPC-5 exhibited the higher catalytic performance than others.

Consequently, Al-SPC-5 was chosen as the catalyst for the following study.

3.3 Recyclability of catalysts

Since Al-SPCs showed rather high catalytic activity and green chemistry principle, its reusability appeared much more important. After completion of the reaction, the catalyst was recovered by filtration, washed with ethanol and acetone, and air-dried. The recovered catalyst was reused in subsequent runs and the results are listed in Table 4. It can be clearly found that only slight decrease of bisphenol F yield were observed after the sixth run, indicating that acid sites did not largely losses during the repeated process. In order to confirm the above speculation, the recovered Al-SPC-5 was explored using NH_3-TPD, XRD, and FT-IR. XRD of the fresh and recovered catalyst Al-SPC-5 after six times listed in Fig. 8 (A). It clearly find that the intensity of 001 reflection peak is decrease. Moreover, the 001 reflection peak is shifted toward higher diffraction angles after the six cycle. The reason for this result may be that reactants and trimer adsorbed on the clay layers after the six cycle, and resulting in reduced basal spacings. NH_3-TPD spectra of sixth repeated used Al-SPC-5 were analyzed to further confirm the acid property of recycled catalysts, and the results are presented in Fig. 8 (B). As compared with the fresh catalyst, slight decrease in the moderate acid sites' peaks intensity of the recovered catalyst Al-SPC-5 after six times was observed. It is attributed to the acid site adsorption of some compounds, resulting in a reduction in the amount of acid sites after the six cycle.

Table 3. Catalytic activities of MMT, SPC, Al-SPCs and Al-MMT for bisphenol F[a]

			Isomer distribution/%		
Catalyst	Yield/%	Selectivity/%	4,4'-Isomer	2,4'-Isomer	2,2'-Isomer
MMT	10.2	90.5	18.3	51.2	30.5
SPC	12.3	91.2	20.7	51.1	28.2
Al-SPC-1	36.5	97.6	27.4	51.3	21.3
Al-SPC-3	72.8	97.2	29.1	50.8	20.1
Al-SPC-5	95.4	98.2	29.6	50.2	20.2
Al-SPC-7	94.7	98.1	29.3	50.1	21.6
Al-MMT	87.3	90.4	32.2	48.5	19.3

[a] Reaction conditions: phenol/formaldehyde molar ratio, 15:1; catalyst concentration, 0.003 g/g; reaction temperature, 353 K; reaction time, 40 min.

View Article Online
DOI: 10.1039/C6RA15161B

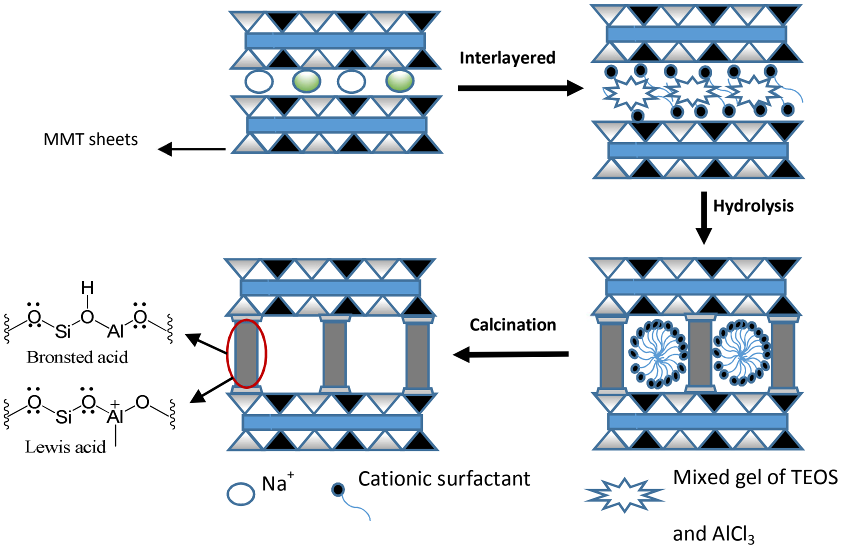

Scheme 2. Schematic for preparation of Al-containing mesoporous silica-pillared clay.

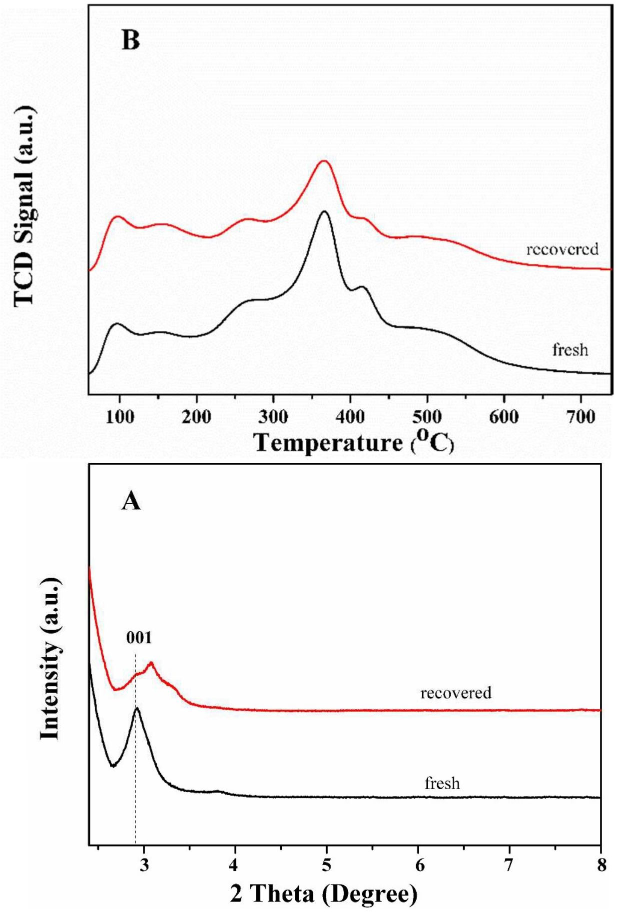

Fig. 8 Small XRD patterns (A) and NH_3-TPD profile (B) of fresh and recovered Al-SPC-5 after six times.

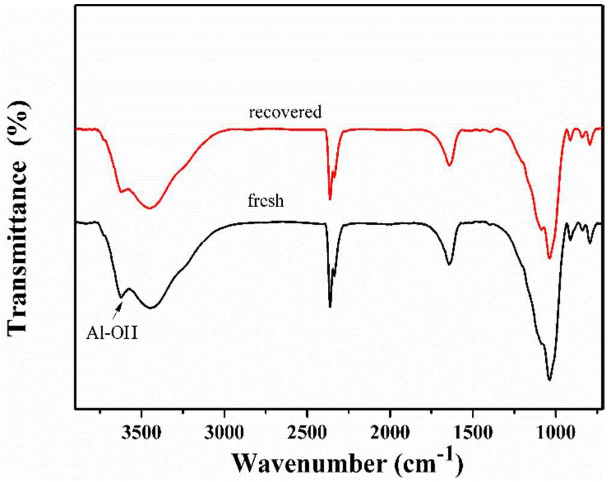

Fig. 9 FT-IR spectra of fresh and recovered Al-SPC-5 after six times.

In order to further explain the superior recyclability of Al-SPCs, the FT-IR spectrum of the sixth repeated used Al-SPC-5 was compared with that of the fresh Al-SPC-5, and the results are shown in Fig. 9. As compared with the spectrum of the fresh Al-SPC-5, slight decrease of the peak intensity at 3652 cm^{-1} (corresponding to the Al–OH, which is acid site) in the spectrum of the recovered Al-SPC-5. This is well agreement with the result that the yield shows slight decrease after the sixth run. These results clearly showed that the Al-SPCs had the great potential to be effectively separated and reused for the hydroxyalkylation of phenol.

3.4 Optimization of Reaction Parameters.

The effects of the phenol/formaldehyde molar ratio (3, 5, 10, 15, and 20) on the yield, selectivity, and the isomers' distribution of bisphenol F over Al-SPC-5 are illustrated in Fig. 10. The product yield is increased significantly from 48 to 95% with a change in the phenol/formaldehyde ratio from 3 to 15; With further increase in mole ratio of the phenol/formaldehyde to 20, both the yield and selectivity of bisphenol F does not any significant changes. This was

View Article Online
DOI: 10.1039/C6RA15161B

Table 4. Catalytic activities of Al-SPC-5 recycled different numbers of times.

			Isomer distribution/%		
Cycle no	Yield/%	Selectivity/%	4,4'-Isomer	2,4'-Isomer	2,2'-Isomer
0	95.4	98.2	27.3	50.6	22.1
1	94.1	97.5	27.5	50.2	22.3
2	93.3	97.1	28.2	51.3	20.5
3	93.1	97.0	28.4	50.5	21.1
4	92.0	97.0	29.1	50.8	20.1
5	91.4	96.4	28.6	50.1	21.3
6	91.2	96.4	28.1	50.7	21.2

mainly because of the blockage of active sites of the catalyst by more phenol molecules present in excess amount for a mole ratio of 20.[32] Moreover, when increasing phenol concentration, the formaldehyde molecules can be surrounded by phenol molecules that resulting in the initially formed bisphenol F molecules to almost not contact the formaldehyde molecule to form higher homologues.[33] The selectivity of the 4,4′ and 2,4′-isomer increases from 26 to 28% and from 46 to49%, whereas the selectivity of the 2,2′-isomer decrease from 29 to 23% .Thus, the optimal molar ratio was 15.

Fig. 11 shows the effect of catalysts concentration on the yield, selectivity, and isomers' distribution of bisphenol F. As shown in Fig.11, the product yield dramatically increased from 75 to 95% upon increasing the catalyst concentration increased from 0.0005 to 0.003 g/g. Nevertheless, further increase in catalyst concentration, the product yield remained almost unchanged. This may be attributed to this reason that overused catalysts were also beneficial for accelerating the side-reaction to produce more byproducts. Interestingly, No significant changed was observed in the selectivity to bisphenol F and isomer distribution, as increase the catalyst concentration from 0.0005 to 0.003 g/g. Thus, 0.003 g/g was selected as the suitable catalyst dose.

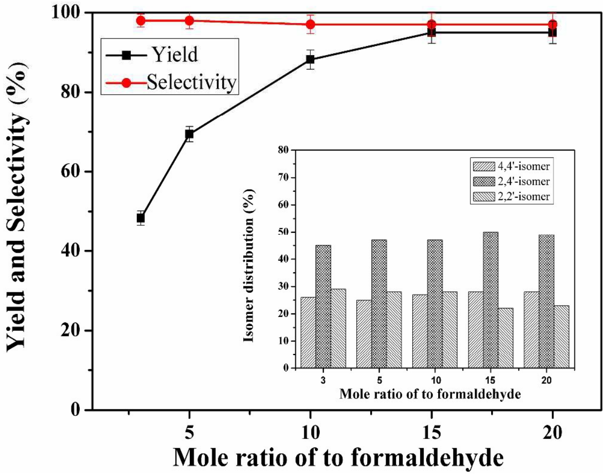

Fig. 10 Effect of phenol/formaldehyde molar ratio on yield, selectivity and isomers' distribution of bisphenol F. Reaction conditions: catalyst, Al-SPC-5; reaction time, 40 min; reaction temperature, 343 K; catalyst concentration, 0.003 g/g.

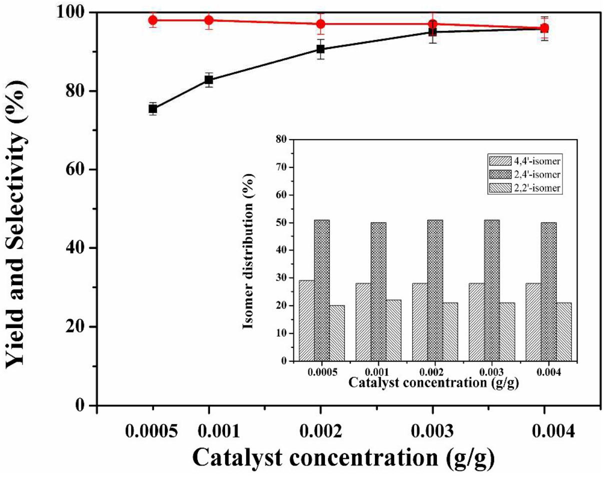

Fig. 11 Effect of catalyst concentration on the yield, selectivity and isomers' distribution of bisphenol F. Reaction conditions: catalyst, Al-SPC-5; mole ratio of phenol/formaldehyde, 15; catalyst concentration, 0.0005–0.004 g/g; reaction time, 40 min; reaction temperature, 343 K.

Results showing the effects of the reaction temperature on product yield, selectivity to bisphenol F and isomer distribution over Al-SPC-5 were investigated and presented in Fig. 12. It was clearly observed that the product yield is significantly increased from 52 to 95%, while the bisphenol F selectivity just changes slightly, ranging from 98 to 97% with increased temperature from 313 to 343 K. However, further increase in temperature upon to 353 K, the product yield show a contradictory decreasing trend. It has been previously proved that an increase of the reaction temperature may result in the formation of some undesired by products such as trimer. In addition, the selectivity of the 4,4′-isomer decreased from 49 to 32%, However, the selectivity of 2,4′- and 2,2′-isomers increased from 42 to 47% and 9 to 21% , respectively. Thus, 343 K was chosen as the optimal reaction temperature.

The effects of reaction time on the products yield, bisphenol F selectivity and isomers' distribution was also studied and the results are shown in Fig. 13. It was clearly observed that the product yield increases rapidly from 65 to 95%, while remained almost unchanged in bisphenol F selectivity with increased reaction time from 10 to 40 min. When further prolonged reaction time to 50 min, the product

View Article Online
DOI: 10.1039/C6RA15161B

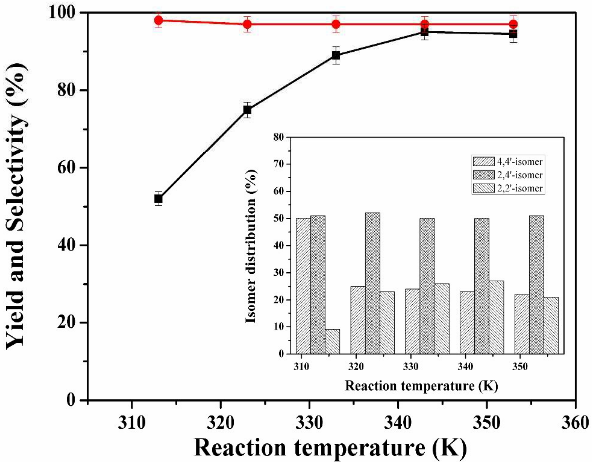

Fig. 12 Effect of reaction temperature on the yield, selectivity and isomers' distribution of bisphenol F. Reaction conditions: catalyst, Al-SPC-5; phenol/formaldehyde, 15; reaction time, 40 min; reaction temperature, 313–353 K; catalyst concentration, 0.003 g/g.

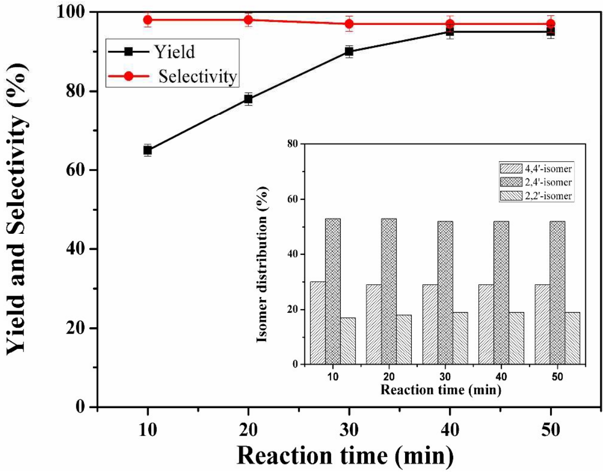

Fig. 13 Effect of reaction time on the yield, selectivity and isomers' distribution of bisphenol F. Reaction conditions: catalyst, Al-SPC-5; mole ratio of phenol/formaldehyde, 15; reaction time, 10–50 min; catalyst concentration, 0.003 g/g.

yield and selectivity to bisphenol F only shows a minor change. This is expected due to the bisphenol F conversion into a trimer as longer reaction time. The selectivity of 4,4′- and 2,4′-isomer decreased from 30 to 28% and 53 to 51%, however, the selectivity of 2,2′-isomers increased from 17 to 20%, respectively. Based on the results, we consider that 40 min is the reaction time for optimal performance.

3.5 Plausible mechanistic pathway.

On the basis of our group previous studies[13] and some relative literature,[33] a plausible catalytic reaction mechanism was proposed and is shown in scheme 3.The synthesis of bisphenol F via the condensation reaction of phenol with formaldehyde is a typical acid-catalyzed reaction.[35] Following the adsorption of the formaldehyde on the Brönsted acid sites, and to form a carbenium ion intermediate (A) by eliminate water. At the same time, the carbenium ion were produced by the abstraction of H^- over Lewis acid sites of the catalyst. Subsequently, the carbenium ion may attack phenol to form para or ortho hydroxy benzyl alcohol (B or C).B or C was activated in the presence of Brönsted acid or Lewis acid to form para or ortho hydroxy benzyl carbonium ion (D or E) and released a water molecule simultaneously. Then, Species D or E with strong electrophillicity attacked the para or ortho carbon atom of an phenol molecule to form 2,2'-isomers, 2,4'-isomers, and 4,4'-isomers of bisphenol F.

It can be found from the entire catalytic process that the catalytic active sites of Al-SPCs are mainly from the hydrogen proton (Brönsted acid) and coordinatively unsaturated Al^{m+} sites (Lewis acid) in the pillars.[31] Rataboul et al.[36] measured Minimum-activation energy required for catalysis by Brönsted and Lewis acid sites, and manifested the protonation of formaldehyde is activated by Lewis acid to capture H^- from the reaction required activation energy is more than Brönsted acid activation energy required. Meanwhile, we find that catalysts with high Lewis to Brönsted acid site ratios resulted in higher catalytic activity, which are confirmed by the results of Py-IR. It means that the hydroxyalkylation of phenol to bisphenol F is catalyzed by the synergy of Brönsted acid and Lewis acid rather than a single one. These results are also in qualitative agreement with the experimental work of Weingarten and co-workers.[37]

4. Conclusions

Mesoporous Al-SPCs with different Al content were prepared in the presence of cationic surfactant by structure-directing method. These materials possess mesoporous structure with large specific surface areas. The incorporated Al leading to the increase and redistribution of Brönsted and Lewis acid sites on SPC. These catalysts show excellent catalytic activity and selectivity to bisphenol F. The sufficient moderate acid sites and high surface area are critical for achieving the highest yield and selectivity of bisphenol F in hydroxyalkylation of phenol. Moreover, the reusability of the catalyst was studied, the results showed that the catalysts can be recovered for at least six times without significant loss of their catalytic activities. In addition, the influences of various reaction parameters like mole ratio, catalyst concentration, reaction temperature and reaction time on the product yield and selectivity to bisphenol F were investigated and a plausible mechanistic pathway was proposed.

Acknowledgements

This research was financially supported by the National Natural Science Foundation of China (no. 51378187, J1210040), Innovative Research Team Development Plan-Ministry of Education of China (no. IRT1238), the Key Project of Hunan Provincial Education Department (no. 13CY001), and Hunan Provincial International Cooperation Project of China (no. 2014WK3030).

View Article Online
DOI: 10.1039/C6RA15161B

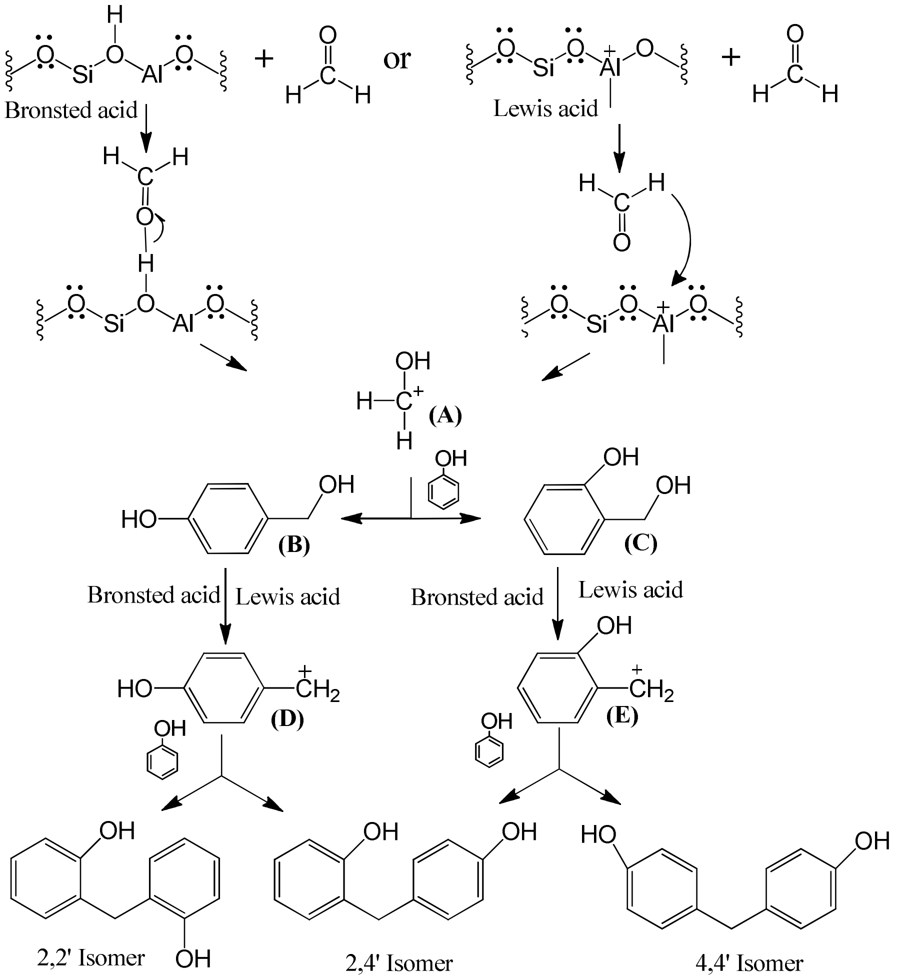

Scheme. 3 Proposed plausible mechanism for hydroxyalkylation of phenol and formaldehyde to bisphenol F.

Notes and references

1 M. Okihama and J. Kunitake, Patent JP 09067287, 1997.
2 S. K. Jana, T. Kugita, and S. Namba, *Catal. Lett*., 2003, **90**,3-4.
3 R. Liu, X. Niu, X. Xia, Z. Zeng, G. Zhang and Y. Lu, *RSC Adv*., 2015, **5**, 62394-62401.
4 N. Maksimchuk, M. Timofeeva, M. Melgunov, A. Shmakov, Y. Chesalov, D. Dybtsev, V. Fedin and O. Kholdeeva, *J.Catal.,* 2008, **257**, 315-323
5 K. Nowinska, W. Kaleta, *Appl. Catal. A*, 2000,**203**, 91–100.
6 M. Chen, J. Yan, Y. Tan, Y. Li, Z. Wu, L. Pan and Y. Liu, *Ind. Eng. Chem. Res.,* 2015, **54**, 11804-11813.
7 A. C. Garade, V. S. Kshirsagar and C. V. Rode, *Appl. Catal. A*, 2009, **354**, 176-182.
8 M. A. De Leon, M. Sergio, J. Bussi, G. Ortiz de la Plata, A. E. Cassano and O. M. Alfano, *Ind. Eng. Chem. Res.,* 2015, **54**, 1228-1235.
9 J. Virkutyte and R. S. Varma, *ACS Sustainable. Chem. Eng.,* 2014, **2**, 1545-1550.
10 C. D. Keenan, M. M. Herling, R. Siegel, N. Petzold, C. R. Bowers, E. A. Rossler, J. Breu and J. Senker, *Langmuir.,* 2013, **29**, 643-652.
11 H. Mao, B. Li, X. Li, L. Yue, J. Xu, B. Ding, X. Gao and Z. Zhou, *Microporous Mesoporous Mater.,* 2010, **130**, 314-321.
12 S. Yang, G. Liang, A. Gu and H. Mao, *Ind. Eng. Chem. Res.,* 2012, **51**, 15593-15600.
13 X. Wu, X. Xia, R. Liu and Y. Chen, *RSC Adv.,* 2016, **6**, 34625-34632.
14 Q, Hao, G, Wang, Z, Liu, J, Lu, and Z, Liu, *Ind. Eng. Chem. Res.*,2010, **49**, 9004–9011.
15 A. Gil, R. Trujillano, M. A. Vicente, and S. A. Korili, *Ind. Eng. Chem. Res.,* 2008, **47**, 7226–7235.
16 H.Mao, B, Li, X Li, L. Yue, Z. Liu, and W. Ma, *Ind. Eng. Chem. Res.*, 2010, **49**, 583–591.
17 Y. Gao, Y. Guo and H. Zhang, *J Hazard Mater.,* 2016, **302**, 105-113.
18 F. Tomul, *Ind. Eng. Chem. Res.*, 2011, **50**, 7228-7240.
19 H. Mao, B. Li, X. Li, Z. Liu and W. Ma, *Mater. Res. Bulletin.,* 2009, **44**, 1569-1575.
20 Y. Han, H. Matsumoto, and S. Yamanaka, *Chem. Mater.,* 1997, **9**, 2013-2018.

View Article Online
DOI: 10.1039/C6RA15161B

21 H. Mao, B. Li, X. Li, Z. Liu, W. Ma, *Materials Research Bulletin.,* 2009,**44**, 1569–1575.

22 S. G.Hur, T. W. Kim, S.J. Hwang, S.H.Hwang, J. Yang, and J.H. Choy, *J. Phys. Chem. B,* 2006, **110**, 1599-1604.

23 J.H. Choy, H. Jung, Y.S. Han, J.B. Yoon, Y.G. Shul, and H.J. Kim, *Chem. Mater.*, 2002, **14**, 3823-3828.

24 M. A. Vicente, C. Belver, M. Sychev, R. Prihod'ko, and A. Gil, *Ind. Eng. Chem. Res.*,2009, **48**, 406–414.

25 J. Valverde, A.Lucas, F. Dorado, A. Romero, and P. Garcı ´a, *Ind. Eng. Chem. Res.*, 2005, **44**, 2955-2965.

26 M. Balaraju, V. Rekha, P. S. S. Prasad, B. L. A. P. Devi, R. B. N. Prasad and N. Lingaiah, *Appl. Catal. A*, 2009, **354**, 82-87.

27 G. Centi, S. Perathoner, F. Trifirb, *J. Phys. Chem.,* 1992, **96**. 2617-2629.

28 F. Chambon, F. Rataboul, C. Pinel, A. Cabiac, E. Guillon and N. Essayem, *Appl. Catal. B*,2011, **105**, 171-181.

29 B. Devassy, F. Lefebvre and S. Halligudi, *J. Catal.,* 2005, **231**, 1-10.

30 A. M. Alsalme, P. V. Wiper, Y. Z. Khimyak, E. F. Kozhevnikova and I. V. Kozhevnikov, *J.Catal.,* 2010, **276**, 181-189.

31 H. Mao, B. Li, L. Yue, L. Wang, J. Yang and X. Gao, *Appl. Clay Sci.,* 2011, ***53*****,** 676-683.

32 R. Liu, X. Xia, X. Niu, G. Zhang, Y. Lu, R. Jiang and S. He, *Appl. Clay Sci.,* 2015, ***105-106***, 71-77.

33D. Wang, Z. He, Z. Wu, Y. Tan, Y. Li and Y. Liu, Chinese. J. Chem. Eng, 2016.

34 J. Tian, H. An, X. Cheng, X. Zhao and Y. Wang, *Ind. Eng. Chem. Res.*, 2015, **54**, 7571-7579.

35 Q. Wang, Z. M. Wu, Y. Li, Y. Tan, N. Liu and Y. Liu, *RSC Adv.,* 2014, **4**, 33466- 33473.

36 F. Chambon, F. Rataboul, C. Pinel, A. Cabiac, E. Guillon and N. Essayem, *Appl. Catal. B*, 2011, **105**, 171-181.

37 R. Weingarten, G. A. Tompsett, W. C. Conner and G. W. Huber, *J. Catal.,* 2011, **279**, 174-182.

View Article Online
DOI: 10.1039/C6RA15161B

Mesoporous Al-incorporated silica-pillared clay interlayer materials for catalytic hydroxyalkylation of phenol to bisphenol F.